RSC Advances

PAPER

View Article Online
View Journal | View Issue

Cite this: *RSC Adv.*, 2022, **12**, 35358

Functionalized aliphatic polyketones with germicide activity†

Esteban Araya-Hermosilla, [a] Paola Parlanti, [a] Mauro Gemmi, [a] Virgilio Mattoli, [a] Sebastiano Di Pietro, [b] Dalila Iacopini, [b] Carlotta Granchi, [b] Barbara Turchi, [c] Filippo Fratini, [c] Valeria Di Bussolo, [b] Filippo Minutolo, [b] Francesco Picchioni [d] and Andrea Pucci *[e]

Received 11th October 2022
Accepted 2nd December 2022

DOI: 10.1039/d2ra06396d

rsc.li/rsc-advances

The COVID-19 pandemic has further confirmed to the community that direct contact with contaminated surfaces and objects represents an important source of pathogen spreading among humans. Therefore, it is of paramount importance to design effective germicidal paints to ensure a rapid and potent disinfectant action of surfaces. In this work, we design novel germicide polymeric coatings by inserting quaternary ammonium and sugar groups on the macromolecular backbone, thus respectively endowing the polymer with germicide features and hydrophilicity to interact with the surfaces. An aliphatic polyketone was selected as a starting polymer matrix that was functionalized with primary amine derivatives *via* the Paal–Knorr reaction. The resulting polymers were deposited on cellulose filter papers and checkboard charts with excellent coating yield and substrate coverage as determined by scanning electron microscopy for cellulose. Remarkably, the substrates coated by the functional polymers bearing quaternary ammonium compounds showed excellent bactericide properties with antibacterial rate of 99% and logarithmic reduction of >3. Notably, the polymers with higher hydrophobicity showed better retention on the substrate after being treated with water at neutral pH.

Introduction

Germicidal coatings have so far proved able to kill viruses and bacteria on commonly utilized objects for relatively long periods of time, and include inorganic nanoparticles,[1–3] antimicrobial peptides,[4] and polymeric cations.[5–8] In particular, the effectiveness of quaternary ammonium compounds (QACs) as cationic antimicrobials is well known and applied within several industrial processes. Antimicrobial action of QACs is based on the interaction between positively charged QACs and negatively-charged bacterial cell surfaces through hydrophobic and electrostatic attraction. Once they enter the bacterial cell, QACs replace Ca^{2+} and Mg^{2+} ions from the cytoplasmic membrane to maintain charge neutrality within it. Consequently, the bacterial cytosol is destabilized by the insertion of the hydrophobic tails into the hydrophobic bacterial membrane. This leads to the loss of the proton motive force and eventually to the lysis of bacterial cell.[9] A wide body of knowledge is available on the antibacterial activity of QACs when employed in several types of coatings applied on different surface such as cotton,[10] silicone rubber,[11] and metallic substrates.[12]

Furthermore, quaternary ammonium compounds are well known to have a broad spectrum of activity against enveloped viruses, such as coronaviruses (including SARS-CoV-2), since they act as cationic surfactants that mechanically detach the viral envelope.[13]

Therefore, the search for efficient germicide paints, which may guarantee a rapid, and potent disinfectant action, still is a very lively field of scientific research.

In this work, we aimed at developing innovative multifunctional polymeric materials, containing both germicide and polar moieties in their molecular structures. Based on our experience in the synthesis of functionalized polyketones,[14–18]

[a]*Center for Materials Interfaces @SSSA, Istituto Italiano di Tecnologia, Viale Rinaldo Piaggio 34, Pontedera (PI) 56025, Pisa, Italy*

[b]*Dipartimento di Farmacia, Università di Pisa, Via Bonanno 33, 56126 Pisa, Italy*

[c]*Dipartimento di Scienze Veterinarie, Viale delle Piagge 2, 56124 Pisa, Italy*

[d]*Department of Chemical Product Engineering, Engineering and Technology Institute Groningen (ENTEG), University of Groningen, Nijenborgh 4, 9747AG Groningen, The Netherlands*

[e]*Dipartimento di Chimica e Chimica Industriale, Università di Pisa, Via Moruzzi 13, 56124 Pisa, Italy. E-mail: andrea.pucci@unipi.it; Tel: +39 0502219270*

† Electronic supplementary information (ESI) available: Fig. S1. ^{1}H-NMR spectrum of 2,3,4-triacetoxy-6-tosyl-α-methyl-D-glucopyranoside (**2**). Fig. S2. ^{1}H-NMR spectrum of 2,3,4-triacetoxy-6-azido-α-methyl-D-glucopyranoside (**3**). Fig. S3. ^{1}H-NMR spectrum of **DPS11**. Fig. S4. Model reaction of 2,5-hexanodione with DMP (Pyrrol-DMP). Fig. S5. Pyrrol-DMP quaternized with 1-bromododecane. Fig. S6. SEM micrographs of Leneta coated with the functionalized polyketones. (a) Neat Leneta. Coated with (b) **PK**, (c) **PK1**, (d) **PK2**, (e) **PK3**, and (f). **PK4**. Fig. S7. SEM micrographs of Leneta coated with the functionalized polyketones after water treatment. (a) Neat Leneta. Coated with (b) **PK**, (c) **PK1**, (d) **PK2**, (e) **PK3**, and (f). **PK4**. See DOI: https://doi.org/10.1039/d2ra06396d

we inserted quaternary ammonium groups on polyketone to make it able to kill pathogens and, at the same time, sugar portions to increase its hydrophilic properties on cellulose-based materials, such as paper objects and surfaces. These functional copolymers were prepared by grafting the new moieties on a perfect alternating aliphatic polyketone *via* the Paal–Knorr reaction. We evaluated the success of the chemical modification on polyketone by ^{1}H-NMR and ATR-FTIR, the quantity of the new moieties grafted on the polymer by elemental analysis, and the hydrophilicity of the resulting polymers by contact angle. Finally, supports made of cellulose filter paper or Leneta checkboard chart were coated with these functionalized polymers and submitted to bacterial growth assays.

Results and discussion

Polyketone functionalized with DMP groups *via* the Paal–Knorr reaction

We prepared a functional polyketone with ternary amines groups (**PK1**) by the chemical modification of polyketone (**PK**) *via* the Paal–Knorr reaction with 3-(dimethylamino)-1-propylamine (DMP). The functionalization of polyketone yielded a conversion (C_{co}) of 25.4% estimated from elemental analysis (Table 3 Experimental section). The total di-carbonyl efficiency was calculated (x + y), where x and y are the di-ketone and pyrrolic moles after conversion, respectively (details in polyketone modification with DMP (**PK1**), Experimental section). We used the relative content of nitrogen in the products calculated by elemental analysis.

The functionalization of **PK** with DMP (**PK1**) was confirmed by ATR-FT-IR and ^{1}HNMR spectroscopies. Fig. 1a shows the ATR-FTIR spectrum of **PK** (green) and **PK1** (red). After the Paal–Knorr reaction has occurred, the intensity of the carbonyl group signal (1700 cm^{-1}) decreases, due to the disappearance of the 1,4-dicarbonyl moieties after the Paal–Knorr reaction. Moreover, three weak signals emerged between 1500 to 1600 and at 710 cm^{-1} corresponding either to stretching of the C=N and C=C bonds or both and the C–H out of plane bend of the pyrrole ring, respectively. Finally, stretching bands of the aliphatic C–H of **PK** backbone and functional groups appeared between 2969 and 2873 cm^{-1}.

Fig. 1b shows the ^{1}H-NMR spectra of **PK** before and after functionalization. The signals of the functionalized polymer (**PK1**) correspond to those belonging to the model compound described in the Experimental section. The success of the amine grafting onto the polymer is indicated by the proton signals at 5.75 (H1), 1.98 (H2), and 3.78 (H3) ppm attributed to the pyrrole ring formed during the Paal–Knorr reaction, the methyl group, and methylene groups adjacent to it, respectively. The methylene protons of the functional groups were assigned at 3.78 (H6) and 1.76 ppm (H5), and the proton of the methyl group adjacent to the ternary amine at 2.23 ppm (H7), whereas the remaining signals around 1.0 ppm and at 3.68 ppm (H4) were attributed to the unreacted **PK** aliphatic part comprised of 30 mol% ethylene and 70 mol% propylene.

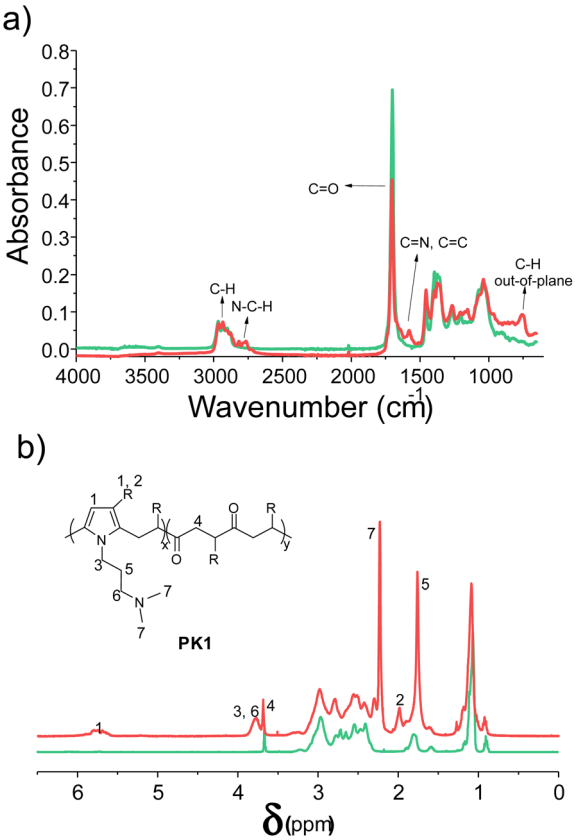

Fig. 1 (a) ATR-FT-IR and (b) ^{1}H-NMR spectra of **PK** (green) functionalized with DMP, **PK1** (red).

Tetra alkyl ammonium moieties were introduced on the **PK1** backbone by the reaction of the amine pendant groups with 1-bromododecane to produce **PK2**. The reaction's success was verified with ATR-FT-IR and ^{1}H NMR spectroscopies. The ATR-FT-IR spectrum of **PK2** (blue line) did not evidence any variation of the main diagnostic absorptions (Fig. 2a). Fig. 2b shows the ^{1}H-NMR spectra of **PK2** (blue line). The polymer shows two new protons signals belonging to the aliphatic chain of 1-bromododecane at 1.27 ppm (methylene groups, H7) and 0.90 ppm (methyl groups, H8). In addition, the methyl protons adjacent to the ternary amine changed position from 2.23 to 3.32 ppm (H5) after quaternization. Notably, all the diagnostic signals were assigned using the model compound described in the Experimental section.

PK2 modification with DPS11 or DPS12

We further functionalized the **PK2** with two sugar derivatives, **DPS11** and **DPS12**, *via* the Paal–Knorr reaction to produce **PK3** and **PK4**, respectively (Fig. 12 Experimental section). The second functionalization on polyketones yielded a carbonyl conversion (C_{co}) of 6.6% and 1.5% for **DPS11** and **DPS12**, respectively. Thus, the overall conversion of **PK3** and **PK4** was 32% and 26.9%, respectively, by considering the C_{co} obtained with DMP (Table 3, Experimental section). The low C_{co} determined after the reaction of the sugar moieties (C_{co} 30% was designed for both

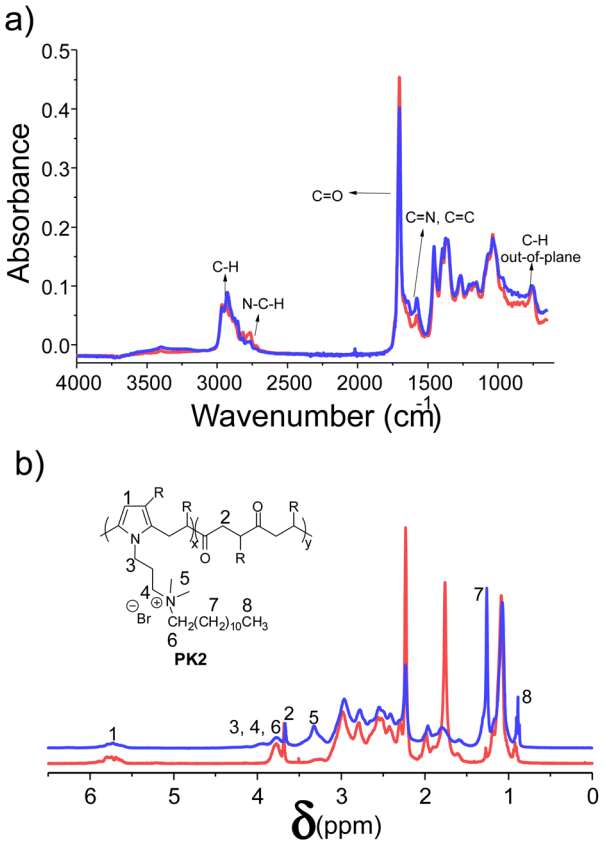

Fig. 2 (a) ATR-FT-IR and (b) ^{1}H-NMR spectra of **PK1** (red) and after amine quaternization with 1-bromododecane (blue).

molecules) can be explained by the limited Paal–Knorr remaining reactivity, and possibly due the important steric hindrance of both DPS reactants and **PK1** after quaternization. Notably, the short connecting aminoalkyl chain in **DPS11** and the acetate groups in **DPS12** diversely contribute in the Paal–Knorr reactivity of the primary amine groups after the functionalization of **PK** with DMP, and also by the steric hindrance produced by the structures and functional groups of and **DPS12**. For instance, the aliphatic chain that connects the primary amine and the aldose in **DPS11** is short to provide an effective interaction between the primary amine and the carbonyl groups belonging to **PK**. In the case of **DPS12**, it displays a longer aliphatic chain that connects the aldose moiety with the primary amine compared to **DPS11**. However, the acyl groups on its aldose moiety probably increase the steric hindrance.

PK3 and **PK4** were characterized by ATR–FTIR and ^{1}H NMR spectroscopies. Fig. 3 shows the ATR-FT-IR spectra of the polymers. The intensity of the carbonyl group signal (1700 cm^{-1}) decreased, due to the further reduction of the number of the 1,4-dicarbonyl moieties after the Paal–Knorr reaction with **DPS11** (**PK3**) and **DPS12** (**PK4**). Furthermore, a broad peak appears in the range of 3600–3000 cm^{-1}, which can be assigned to hydrogen bonding due to the presence hydrogen donor and acceptors groups belonging to the sugar moieties (OH and acyl groups). The appearance of the hydrogen bond peak, together with the decrease in intensity of the signal associated with the

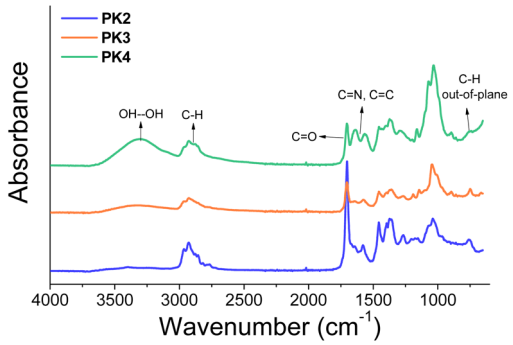

Fig. 3 ATR-FT-IR spectrum of **PK2**, **PK3** and **PK4**.

PK carbonyl, indicate the successful modification of the **PK2** with the sugar moieties. The polymers also show the weak signal between 1500 to 1600 cm^{-1} corresponding either to stretching of C=N and C=C bonds of the pyrrole ring and the stretching C–H bands at 2969 and 2873 cm^{-1} of **PK** backbone, DMP, and 1-bromododecane.

Fig. 4 shows the ^{1}H NMR spectra of PKDMP_Br_DPS11 (**PK3**) and PKDMP_Br_DPS12 (**PK4**). The polymers show new peaks between 4 and 5 ppm, which can be associated to the added sugar portions and, in particular, to: (a) the anomeric protons of both **DPS11** and **DPS12**; (b) the hydroxy groups of **DPS11**; (c) the

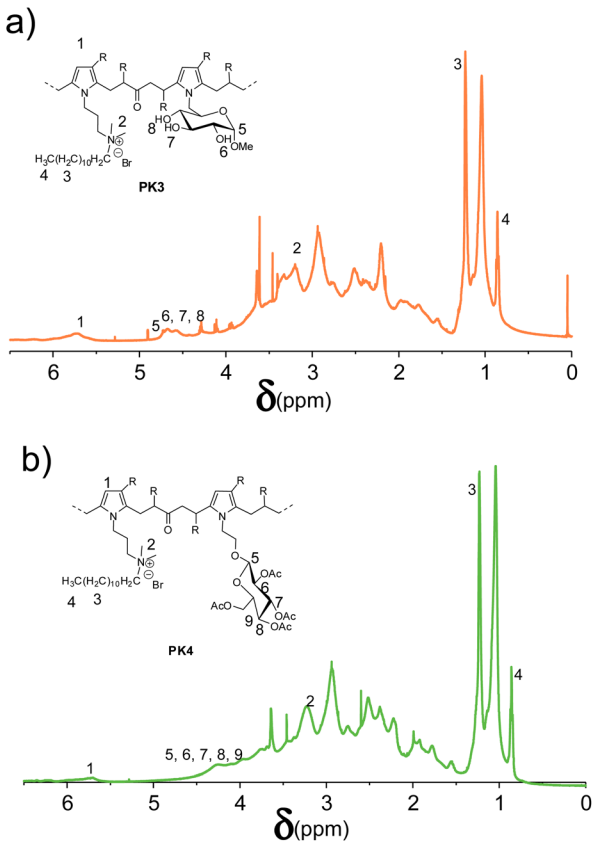

Fig. 4 ^{1}H-NMR spectra of **PK2** modified chemically with (a) **DPS11** (**PK3**) and (b) **DPS12** (**PK4**).

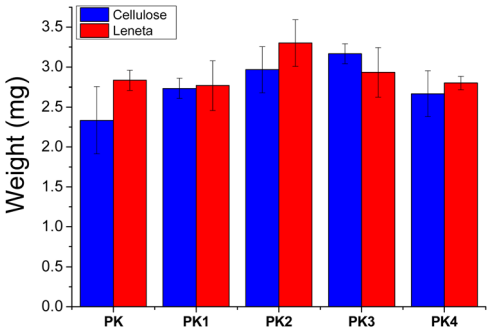

Fig. 5 Weight amounts of the deposited polymers on cellulose and Leneta substrates.

protons in the alpha positions to the acetate groups **DPS12**. All these data confirm the proper functionalization of the polymers with the indicated sugar moieties.

Characterization of functionalized polyketone coatings

We evaluated the affinity of the polymers to the substrates as a function of the nature of their functional groups. Notably, the amount of the material deposited on either the cellulose or the Leneta substrate was determined by weighting the substrate before and after the polymer deposition. Regardless the nature of the polymers, all the coatings showed average weight values close to the theoretical one (3 mg) and within the experimental error (Fig. 5).

The structure of the coating on the substrates were evaluated by SEM. Notably, samples made by Leneta chart did not show any distinguished differences before and after coating with the functionalized **PK** (Fig. S6†). On the other hand, cellulose was a suitable substrate to be analyzed by SEM due to its characteristic fibrous structure (Fig. 6a). All the coatings showed a good affinity for cellulose as indicated by the evenly distributed film that covered the cellulose's fibers (Fig. 6b–f).

Static contact angles (θ) were measured in all coatings on Leneta chart and compared with the bare substrate using water at pH 7.2 as the solvent (Table 1). The samples based on the cellulose substrate were not considered being unsuitable for the present experiment. θ values were collected and compared after 140 seconds, *i.e.*, after reaching a stable and nonfluctuating measurement. As expected from their chemical composition, all the amine-functionalized polyketones provided coatings with progressively increased hydrophilicity, *i.e.*, on passing from 70.7° of the bare Leneta chart to 18.7° after coating with **PK1**, and to eventually 3.1° for **PK3**, that is, the polymer containing sugar moieties with free OH groups exposed. On the other hand, the hydrophilicity of **PK4** was partially mitigated by the presence of acetyl groups in the exposed oxygen atoms of the sugar portion. **PK** showed a moderate hydrophilic nature[19] and the quaternization of the **PK1** mitigated the hydrophilicity due to the presence of the long alkyl chain. Overall, the introduction of the carbohydrate moieties into the chain of **PK2** ($\theta = 24.9°$) lead in any case to the generation of more hydrophilic coatings ($\theta = 3.1°$ for **PK3** and $\theta = 19.4°$ for **PK4**), which is logically more pronounced in the case of the "free-OH" analogue **PK3**.

We further evaluated the stability of the coatings after their immersion in deionized water at pH 7.1 for 24 h. To calculate the percentage polymer coating that remained on the substrate after the water immersion, the samples were weighted after drying under vacuum the percentage of retention calculated according to eqn (1).

$$\text{Retention} \quad (\%) = \frac{W_f - W_s}{W_i} \times 100 \qquad (1)$$

where W_f is the weight of the sample after the water immersion, W_s is the weight of the neat substrate, and W_i is the weight of the polymer coating before water immersion.

Fig. 7 shows the percentage of retention of each sample after the water treatment. As expected, the coating made by the more hydrophobic polymer proved to be more resistant to the aqueous washing, showing a better retention on the substrates, in agreement with the results gathered by the contact angle. Unexpectedly, hydrophilic **PK1** showed a good retention on both cellulose and Leneta substrates as well. These results

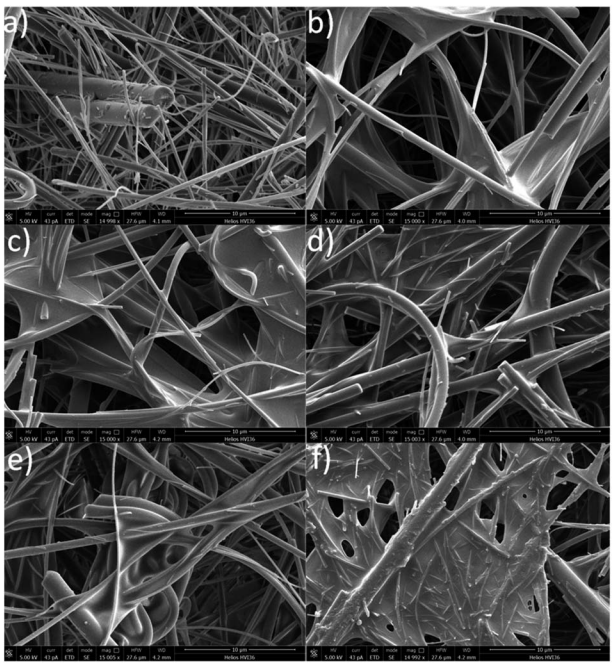

Fig. 6 SEM micrographs of cellulose coated with the functionalized polyketones. (a) Neat cellulose; cellulose coated with (b) PK, (c) PK1, (d) PK2, (e) PK3, and (f) PK4. Scale bar of 10 μm.

Table 1 Contact angle for the polyketones coatings on Leneta checkboard chart

Coatings	θ (°)
Leneta chart	70.7
PK	47.2
PK1	18.7
PK2	24.9
PK3	3.1
PK4	19.4

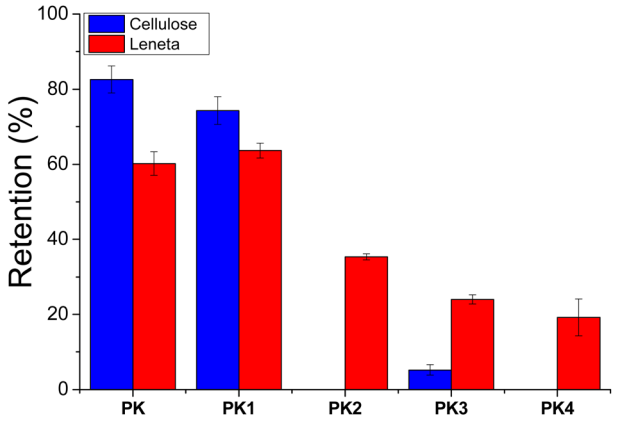

Fig. 7 Percentage of retention of coating after water treatment.

possibly suggest the possibility of the formation of secondary interactions (mainly dipole–dipole) between the tertiary amine moieties with the substrates. Such interactions apparently decreased their extent after **PK1** quaternization, as revealed by the low retention values, especially on the cellulose substrate. Moreover, the high affinity with water of the samples functionalized with the carbohydrate portions of **DPS11** and **DPS12** made their retention on both substrates lower than 20%.

The morphology of the coatings were again evaluated by SEM microscopy after water treatment. Fig. 8 shows the micrographs taken form the cellulose substrate and the results agreed well with those gathered from the retentions (in Fig. S7,† those of Leneta charts were reported). Notably, Fig. 8b and c revealed the retention of **PK** and **PK1** coatings on the cellulose fibers being still covered by a continuous polymer film. Conversely the coatings formed by **PK2** and the sugar-type polymers were almost completely washed out during the water treatment as the micrographs revealed quite a neat cellulose fibrous structure (Fig. 8d–f).

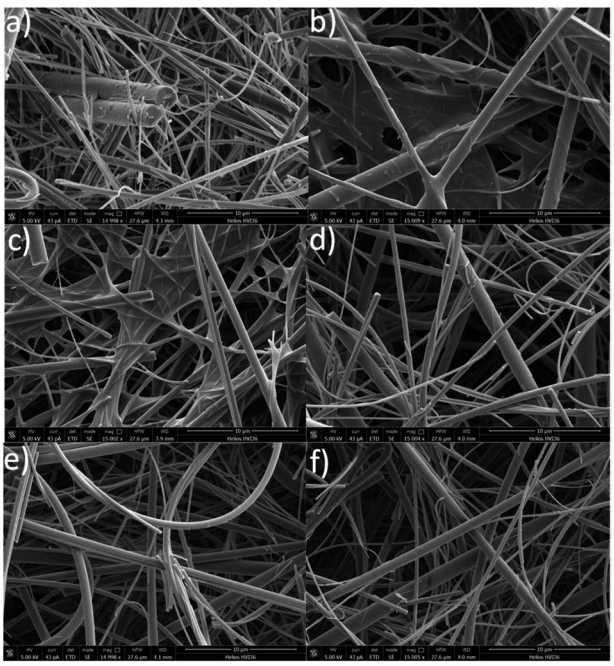

Fig. 8 SEM micrographs of cellulose coated with the functionalized polyketones after the water treatment. (a) Neat cellulose; cellulose coated with (b) **PK**, (c) **PK1**, (d) **PK2**, (e) **PK3**, and (f). **PK4**.

Antibacterial activity assays

S. aureus ATCC6538 was employed as it is recommended for routine screening in antimicrobial susceptibility testing, as well as in trials to assess the evolution of resistance to biocides.[20] Therefore, all the coatings were tested for their ability to inhibit growth of *S. aureus* after incubation for 18 h at 37 °C. The antibacterial rate (*R*%) and the logarithmic reduction were calculated as described in the Experimental section. For each type of coating, three independent replicates were performed, and the results are displayed in Table 2.

Polymers characterized by the presence of QACs in their chains, such as **PK2**, **PK3** and **PK4** showed remarkable antibacterial activities ($R > 99\%$ and log reduction > 3), regardless of their use on different types of surfaces (cellulose or Leneta). The *R* value represent the percentage of dead cells calculated relatively to the control sample growth (CFU mL^{-1}). *R* values higher than 90% are associated to a significant antibacterial activity. On the other hand, the coating lacking QACs (*i.e.*, **PK**) gave no positive results in terms of inhibition of bacterial growth. These data show that the presence of sugar portions attached to the polymer backbone do not interfere with the germicidal action of the quaternary ammonium side chain, since coatings **PK3** and **PK4** displayed no reduction in their antibacterial activities when compared to their non-carbohydrate counterpart, **PK2**.

Experimental

Materials

3-(Dimethylamino)-1-propylamine (DMP), 1-bromododecane and 2,5-hexanodione (Sigma-Aldrich) were purchased and used as received. Aliphatic polyketones made of ethylene, propylene, and carbon monoxide were synthesized according to a reported procedure yielding a polyketone with 30 mol% ethylene and 70 mol% propylene (**PK**) (M_w 2930).[21] **DPS12** was synthesized as previously reported,[22] whereas **DPS11** (ref. 23) was prepared by means of an unprecedented synthetic pathway, as described below (Fig. 9).

Synthesis of DPS11

2,3,4-Triacetoxy-6-tosyl-α-methyl-D-glucopyranoside (2, Fig. 9). In a flame dried modified Schlenk flask 1.0 g of 2,3,4-triacetoxy-α-methyl-D-glucopyranoside[24] **1** (3.12 mmol, 1 eq.) was dissolved in 35 mL of a 1 : 1 mixture of both dry dichloromethane and pyridine under argon atmosphere. The solution was cooled down at 0 °C and 1.0 g of tosyl chloride (5.3 mmol, 1.7 eq.) was added in one portion. The reaction was allowed to reach room temperature and it was kept stirring under argon for 12 h. Then, 3 mL of methanol were added to hydrolyze the excess of tosyl chloride (10 min stirring) and the solution was co-evaporated with toluene. The residual solid was purified by

Table 2 Mean values of *S. aureus* loads (log CFU mL^{-1}) of inoculum, control and different coating samples, antibacterial rate (*R*%) and logarithmic reduction (log CFU mL^{-1})

	Inoculum	Control sample (24 h)	Cellulose untreated (24 h)	Leneta untreated (24 h)	Cellulose **PK** (24 h)	Leneta **PK** (24 h)	Cellulose **PK2** (24 h)	Leneta **PK2** (24 h)	Cellulose **PK3** (24 h)	Leneta **PK3** (24 h)	Cellulose **PK4** (24 h)	Leneta **PK4** (24 h)
log CFU mL^{-1} ± ds	7.6 ± 0.3	5.4 ± 0.2	5.5 ± 0.2	4.9 ± 1.1	5.5 ± 0.1	5.1 ± 0.5	<2	<2	<2	<2	<2	<2
Antibacterial rate (*R*%)	—	—	−25	−106	−13	19	>99	>99	>99	>99	>99	>99
log reduction (log CFU mL^{-1})	—	—	−0.1	0.5	−0.1	0.3	>3	>3	>3	>3	>3	>3

flash chromatography (SiO_2, hexane/ethyl acetate = 6/4) to afford 1.0 g of pure compound **2** (yield = 70%) as a white solid. ^{1}H-NMR (400 MHz, $CDCl_3$) δ (ppm) = 7.78 (d, ^3J = 8.2 Hz, 2H, Ar), 7.35 (d, ^3J = 8.2 Hz, 2H, Ar), 5.42 (t, ^3J = 9.6 Hz, 1H), 4.91 (t, ^3J = 9.8 Hz, 1H), 4.86 (d, ^3J = 3.7 Hz, 1H, anomeric), 4.78 (dd, ^3J = 3.7 Hz and 10.2 Hz, 1H), 4.12–4.05 (m, 2H), 4.03–3.98 (m, 1H), 3.51 (s, 3H, OMe), 2.44 (s, 3H, CH_3–Ar), 2.05 (s, 3H, OAc), 1.98 (s, 3H, OAc), 1.97 (s, 3H, OAc) (S1, ESI†).

2,3,4-Triacetoxy-6-azido-α-methyl-D-glucopyranoside (3, Fig. 9). In a flame dried modified Schlenk flask 600 mg of tosylate 2 (1.26 mmol, 1 eq.) were dissolved in 10 mL of dry DMF and 820 mg of sodium azide (12.6 mmol, 10 eq.) were added. The reaction was kept at 90 °C under argon atmosphere for 12 h. Then, the solution was cooled down at room temperature and filtered from the solid. The solvent was evaporated, and the residual solid was purified by flash chromatography (SiO_2, hexane/ethyl acetate = 6 : 4) to afford 380 mg of compound **3** (yield = 87%) as a white solid. ^{1}H-NMR (400 MHz, $CDCl_3$) δ (ppm) = 5.47 (t, ^3J = 10.2 Hz, 1H), 5.00–4.96 (m, ^3J = 3.7 Hz and 10.2 Hz, 2H, anomeric), 4.88 (dd, ^3J = 3.7 Hz and 10.2 Hz, 1H), 3.98–3.93 (m, 1H), 3.45 (s, 3H, OMe), 3.37–3.26 (m, 2H), 2.07 (s, 3H, OAc), 2.03 (s, 3H, OAc), 2.01 (s, 3H, OAc) (S2, ESI†).

6-Amino-α-methyl-D-glucopyranoside (DPS11, Fig. 9). In a one neck round-bottomed flask 380 mg of compound 3 (1.1 mmol, 1 eq.) were added and dissolved in 70 mL of methanol and 100 mg of Pd on charcoal (10 wt%, 0.056 mmol, 5 mol%). The solution was saturated with hydrogen by means of 3 cycles of vacuum/hydrogen purging and it was kept stirring for 12 h under 1 atm of hydrogen. Then, the product formation was monitored by TLC and the solution was filtered on a Celite pad. To the protected amine solution in methanol (considering a total conversion) 13.5 mL of a 0.33 M solution of MeONa in methanol (4.4 mmol, 4 eq.) were added and the solution was kept stirring at room temperature for 2 h. Then, the excess of methoxide was neutralized with acidic resin Amberlite IR-120, the solution was filtered from the resin and the solvent evaporated to afford 190 mg of pure compound **DPS11** (yield = 90%) as a colorless syrup. ^{1}H-NMR (400 MHz, CD_3OD) δ (ppm) = 4.67 (d, ^3J = 3.8 Hz, 1H, anomeric), 3.60 (t, ^3J = 9.3 Hz, 1H), 3.52–3.46 (m, 1H), 3.41 (s, 2H, NH_2), 3.38 (dd, ^3J = 3.8 and 9.7 Hz, 1H), 3.35 (s, 3H, OMe), 3.14 (t, ^3J = 9.3 Hz, 1H), 2.99 (dd, ^3J = 3.1 and 13.3 Hz, 1H), 2.71 (dd, ^3J = 7.4 and 13.2 Hz, 1H) (S3, ESI†).

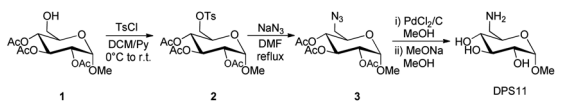

Fig. 9 Schematic representation of the synthesis of **DPS11** (Ac = acetyl, Ts = tosyl, Py = pyridine).

Model compound

A model reaction of 2,5-hexanodione with DMP (pyrrole-DMP Fig. 10a) was prepared intending to assign appropriately the ^{1}H-NMR signals after the Paal–Knorr reaction between polyketone and DMP. The reaction between stoichiometric amounts of DMP and 2,5-hexadione was carried out in a 50 mL round-bottomed flask equipped with a magnetic stirrer, a reflux condenser and a Heat-On™ Block System. First, 2.0 g of 2,5-hexadione (0.018 mol) and 1.79 g of DMP (0.018 mol) were placed in the flask. The reaction was carried out at 80 °C (not solvent) under stirring for 24 h in order to ensure reaction completeness and the reflux condenser was taken the last 5 h to assure the water elimination (by-product of Paal–Knorr reaction). NMR data are reported as follows: chemical shift, multiplicity, coupling constants (hertz), and location. ^{1}H-NMR (400 MHz δ, $CDCl_3$): 1.81 ppm (dt, 2H, J = 14.5, CH_2), 2.27 ppm (s, 6H, CH_3 next to pyrrole and s, 6H, CH_3 next to ternary amine), 2.34 ppm (t, 2H, J = 7.1, CH_2 next to ternary amine), 3.81 ppm (t, 2H, J = 17.3, CH_2 next to pyrrole), 5.8 ppm (s, 2H, pyrrole) (S4, ESI†).

Model compound alkylation with 1-bromododecane

After the synthesis of pyrrole-DMP, the ternary amine pendant group were quaternized by reacting with 1-bromododecane

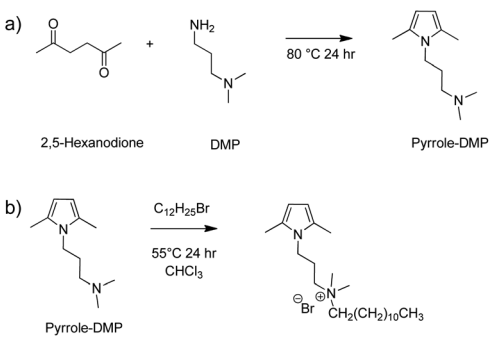

Fig. 10 (a) Model reaction of 2,5-hexanodione with DMP (pyrrole-DMP) and (b) its ternary amine's quaternization.

(Fig. 10b). Therefore, 1 g of pyrrole-DMP (5.6 mmol) and 1.4 g of 1-bromododecane (5.6 mmol mol) were placed in a 50 mL round-bottomed flask equipped with a magnetic stirrer and a Heat-On™ Block System. The reaction was carried out at 55 °C under stirring for 24 h to ensure reaction completeness. NMR data are reported as follows: chemical shift, multiplicity, coupling constants (hertz), and location. ^{1}H-NMR (400 MHz δ, $CDCl_3$): 0.88 (t, 3H, $J = 6.6$, CH_3) 1.27 ppm (d, 20H, $J = 12$, CH_2), 2.24 ppm (s, 6H CH_3–pyrrole), 3.37 ppm (s, 6H, CH_3 next to quaternized amine), 3.55–3.82 ppm (m, 4H, CH_2 next to quaternized amine), 3.93 ppm (t, 2H, $J = 6.8$, CH_2 next to pyrrole), 5.76 ppm (s, 2H, pyrrole) (S5, ESI†).

Polyketone modification with DMP (PK1)

The functionalization of **PK** with DMP (**PK1**, Fig. 11a) was carried out aiming to reach 35% of polyketone's di-carbonyl groups conversion (Table 3). First, 5 g of **PK** were placed in a 50 mL round-bottomed flask equipped with a magnetic stirrer, a reflux condenser and a Heat-On™ Block System. Afterward, 1.7 mL of DMP was added to the polymer solution dropwise for 5 min. After the 5 min, the reaction was carried out at reflux for 3 h and the condenser was taken of the last hour. The product dissolved with chloroform and purified by solvent extraction with brine. The process was repeated three times to remove any unreacted amine and the organic solvent was removed by evaporation. The carbonyl conversion (C_{co}), *i.e.*, the molar fraction of 1,4-dicarbonyl units reacted *via* the Paal–Knorr reaction, was calculated on the basis of elemental analysis as the following:

$$C_{co} = \frac{y}{y + x} \times 100\% \quad (2)$$

where x and y are the di-ketone and pyrrolic moles after conversion, respectively. y was determined as follows:

$$y = \frac{\mathrm{wt(N)}}{A_m(\mathrm{N})} \quad (3)$$

where wt(N) are the grams of N of the product as determined by elemental analysis and A_m(N) is the atomic mass of N. x was then determined as follows:

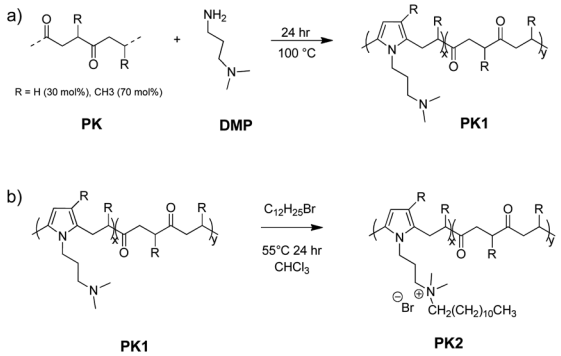

Fig. 11 Schematic representation of the polyketone functionalization with DMP (**PK1**) and the successive alkylation of the pending amine groups (**PK2**).

Table 3 Elemental analysis of **PK** and **PK** functionalized with DMP, **DPS11**, or **DPS12**

Sample	x^a (%)	y^b (%)	z^c (%)	$C_{co}{}^d$ (%)
PK	100	—	—	—
PK1	74.6	25.4	—	25.4
PK3	68.0	25.4	6.6	32.0
PK4	73.1	25.4	1.5	26.9

[a] Moles percentage of di-ketone groups in the polymer (x). [b] Moles percentage of ternary amine groups in the polymer (y). [c] Moles percentage of sugar moieties groups in the polymer (z). [d] Total di-carbonyl conversion (C_{co}, %) after double functionalization as obtained from EA as described for **PK1**.

$$x = \frac{g_{prod} - y \times M_w^y}{M_w^{pk}} \quad (4)$$

where g_{prod} is the gram of the product, M_w^y the molecular weight of the pyrrolic unit and M_w^{pk} the molecular weight of a 1,4 di-ketone unit. From the ratio between C_{co} and the corresponding amount in alimentation (C_{co}^{feed}), the conversion efficiency η can be calculated as the following:

$$\eta = \frac{C_{co}}{C_{co}^{feed}} \times 100\% \quad (5)$$

where C_{co}^{feed} corresponds to:

$$C_{co}^{feed} = \frac{\mathrm{Mol_{amine}}}{\mathrm{Mol_{d\text{-}CO}}} \times 100\% \quad (6)$$

With $\mathrm{mol_{amine}}$ are the moles of amine and $\mathrm{mol_{d\text{-}CO}}$ the moles of di-carbonyl units in alimentation.

In order to adjust the stoichiometry of the functional groups, a polymer molecular weight (PMW) of 476.1 g mol^{-1} of ternary amines groups was considered, related with x of 0.254. This is calculated by the following formula:

$$\mathrm{PMW} = \frac{xM_p + yM_c}{x} \quad (7)$$

where y is the fraction of non-converted 1,4-dicarbonyl groups, provided by $x + y = 1$.

Alkylation of PK1 with 1-bromododecane (PK2)

After the functionalization of polyketone, we proceed to alkylate the amine groups of **PK1** (Fig. 11b). First, 3.353 g of **PK1** was dissolve in 50 mL of chloroform and place in a round bottom flask equipped with a stirrer and a reflux condenser and a Heat-On™ Block System. Stoichiometric amounts of 1-bromododecane related to the amine functional groups (formula (7)) were added to the reaction mix. The reaction was carried out during 48 hours at a temperature of 50 °C. The product was dried at reduced pressure for 24 h and the unreacted 1-bromododecane was extracted by dissolving the polymer in methanol and extracting the unreactive 1-bromododecane with hexane (solvent–solvent extraction). Finally, **PK2** was characterized by ^{1}H NMR and ATR-FT-IR.

Polyketone modification with DPS11 (PK3) and DPS12 (PK4)

After the modification of polyketone with DMP (**PK1**) and its quaternization with 1-bromododecane (**PK2**), a second polyketone functionalization was carried out with **DPS11** and **DPS12** (Fig. 12). First, 0.73 g of **PK2** was dissolved in 35 mL of methanol and place in a round bottom flask equipped with a stirrer and a reflux condenser and a Heat-On™ Block System. Then, 0.31 g of **DPS11** were added to the reaction mix to produce **PK3**. The reaction was carried out during 48 hours at a temperature of 60 °C. The dried products dissolved in chloroform and purified by solvent extraction with brine. The process was repeated three times to remove any unreacted **DPS11**. The organic solvent was removed by evaporation. The same procedure was repeated for **DPS12** but changing the amount of reagent to set the same carbonyl conversion as **DPS11** (*i.e.*, C_{co} 30%). Thus, 0.25 g of **DPS12** was added to 0.29 g of **PK2** to produce **PK4**. The products were characterized by ^{1}H NMR and ATR-FT-IR, and the carbonyl conversion (C_{co}) was calculated by elemental analysis as described above.

Fabrication and characterization of the functionalized polyketone coatings

Functionalized polyketones and pristine polyketone were dissolved in chloroform or methanol at a concentration of 50 mg mL^{-1} for 10 minutes under stirring. Then, the coatings were prepared by depositing 60 μL of polymer solution on a 1 cm^2 substrate of cellulose filter paper or Leneta checkboard chart (refer as Leneta). Four different coatings were realized: pristine polyketone (**PK**), polyketone functionalized with DMP (**PK1**), **PK1** after quaternization with 1-bromododecane (**PK2**), and **PK2** functionalized with **DPS11** and **DPS12** (**PK3** and **PK4**, respectively). The amount of polymer coated on the substrates were determined by weighing the substrate before and after the polymer deposition. Each measurement was repeated three times and the average determined with the standard deviation. Their coatings wettability was determined by static contact angle using the sessile drop method (Camtel FTA200 Drop Shape Analyzer with FTA 32 software) at room temperature and with deionized water (pH 7.2) as testing liquid. Additionally, the stability of the coatings was determined by weighting the samples after water immersion in deionized water at pH 7.2. The coatings morphology was observed by scanning electron microscopy (SEM), by using a Dual Beam FIB/SEM Helios NanoLab 600i (FEI), at 10 kV accelerating voltage and variable magnifications. For SEM imaging, the samples were prepared by Au deposition (layer about 40 nm) using AC sputtering.

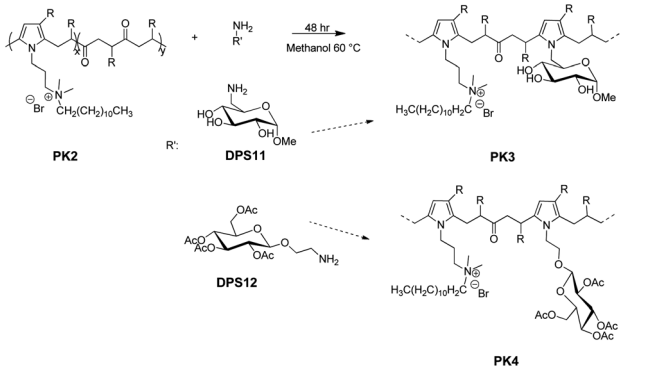

Fig. 12 Schematic representation of the quaternized PKDMP functionalized with DPS11 (PK3) or DPS12 (PK4) *via* the Paal–Knorr reaction.

Antibacterial activity assays

Staphylococcus aureus ATCC6538, added with 15% glycerol as cryoprotective agent, was stored at −80 °C in Brain and Heart Infusion broth (BHI, Thermo Fisher Diagnostics, Milan, Italy). After incubation at 37 °C for 24 hours in BHI broth, the bacterial suspension was centrifuged (6000 rpm, 5 minutes) and bacterial cells were washed with sterile saline solution. To standardize the bacterial inoculum, a bacterial suspension with a turbidity equal to the point 0.5 of the McFarland scale was prepared in sterile saline suspension at approximately 1.5 × 10^8 colony-forming units (CFU) mL^{-1}. An aliquot of standardized inoculum was also collected to enumerate the actual bacterial cell concentration on Mannitol Salt Agar (MSA, Thermo Fisher Diagnostics, Milan, Italy).

To test the polymeric coatings, they were placed on a Petri dish and UV-treated for 10 minutes on each side. Twenty mL of bacterial inoculum were added in each plate. A control plate containing only the inoculum suspension was also included. Plates were incubated at 37 °C in aerobic condition and in agitation (150 rpm) for 18 hours. After incubation, bacterial suspensions and the polymeric coatings were transferred in 50 mL-tubes and vigorously vortexed. An aliquot of each bacterial suspension was collected and serially diluted to determine the staphylococcal cell concentration on MSA (37 °C, aerobic condition, 48 hours). The antibacterial rate (R%) and logarithmic reduction were calculated as described in literature,[25] by applying the following formulas: $(R\%) = (B - C)/B \times 100$; log reduction = $\log B - \log C$; where B is the CFU mL^{-1} of control sample and C is the CFU mL^{-1} of tested samples. For each type of coating, three independent replicates were performed. When the result obtained from the enumeration was under the detection limit (100 CFU mL^{-1}), the arbitrary value of 50 CFU mL^{-1} was assigned.

Conclusions

In conclusion, we have prepared novel functional polymers endowed with germicide activity and polar moieties as pendant groups. The starting material used for this purpose was an aliphatic polyketone, obtained by the polymerization of CO, ethylene, and propylene. Polyketone was readily modified chemically by Paal–Knorr reaction using as reagents primary amine derivatives to introduce quaternary ammonium pendant groups after quaternization, and sugar moieties to increase the hydrophilicity of the polymer and its interaction with the selected substrates. All the functional polymers showed a hydrophilic character with contact angles less than 25 °C specially for the polymer containing with sugar groups.

Remarkably, the substrates coated by the functional polymers bearing quaternary ammonium compounds (**PK2**, **PK3** and **PK4**) showed excellent bactericide properties with antibacterial rate of 99% and the logarithmic reduction >3 log CFU mL^{-1}. Contrarily to our expectations, the polymers functionalized with sugar moieties showed poor affinity to the substrates after being treated with water at neutral conditions. However, the more hydrophobic polymers show better results with values of retention higher than 60%. Overall, the easy and mature chemical modification of polyketones *via* the Paal–Knorr reaction open the way of developing novel germicide coatings.

Author contributions

Conceptualization: Andrea Pucci, Francesco Picchioni, Valeria di Bussolo, Filippo Minutolo. Methodology: Esteban Araya-Hermosilla, Andrea Pucci, Valeria di Bussolo, Filippo Minutolo. Investigation: Esteban Araya-Hermosilla, Paola Parlanti, Sebastiano Di Pietro, Dalila Iacopini, Carlotta Granchi, Barbara Turchi, Filippo Fratini. Data curation: Esteban Araya-Hermosilla and Andrea Pucci. Writing – original draft, Esteban Araya-Hermosilla, Andrea Pucci, Filippo Minutolo. Writing – review & editing, Andrea Pucci, Filippo Minutolo. Funding acquisition: Virgilio Mattoli, Andrea Pucci, Mauro Gemmi. All authors have read and agreed to the published version of the manuscript.

Conflicts of interest

There are no conflicts to declare.

Acknowledgements

The authors thanks to Antonella Manariti for her efforts in contributing to the coating's characterization by infrared spectroscopy.

References

1 N. Tripathi and M. K. Goshisht, *ACS Appl. Bio Mater.*, 2022, **5**, 1391–1463.
2 M. K. Goshisht, *Adv. Mater. Proc.*, 2021, **2**, 535–546.
3 M. T. Matter, M. Doppegieter, A. Gogos, K. Keevend, Q. Ren and I. K. Herrmann, *Nanoscale*, 2021, **13**, 8224–8234.
4 L. Yu, K. Li, J. Zhang, H. Jin, A. Saleem, Q. Song, Q. Jia and P. Li, *ACS Appl. Bio Mater.*, 2022, **5**, 366–393.
5 A. M. Piras, S. Esin, A. Benedetti, G. Maisetta, A. Fabiano, Y. Zambito and G. Batoni, *Int. J. Mol. Sci.*, 2019, **20**, 6297.
6 P. Li, C. Zhou, S. Rayatpisheh, K. Ye, Y. F. Poon, P. T. Hammond, H. Duan and M. B. Chan-Park, *Adv. Mater.*, 2012, **24**, 4130–4137.
7 X. Ding, A. Wang, W. Tong and F. Xu, *Small*, 2019, **15**, 1900999.
8 S. Some, S.-M. Ho, P. Dua, E. Hwang, Y. H. Shin, H. Yoo, J.-S. Kang, D. Lee and H. Lee, *ACS Nano*, 2012, **6**, 7151–7161.
9 L. A. T. W. Asri, M. Crismaru, S. Roest, Y. Chen, O. Ivashenko, P. Rudolf, J. C. Tiller, H. C. van der Mei, T. J. A. Loontjens and H. J. Busscher, *Adv. Funct. Mater.*, 2014, **24**, 346–355.
10 Y. Liu, K. Ma, R. Li, X. Ren and T. S. Huang, *Cellulose*, 2013, **20**, 3123–3130.
11 B. Gottenbos, H. C. van der Mei, F. Klatter, P. Nieuwenhuis and H. J. Busscher, *Biomaterials*, 2002, **23**, 1417–1423.
12 Y. Dong, L. Liu, J. Sun, W. Peng, X. Dong, Y. Gu, Z. Ma, D. Gan and P. Liu, *J. Mater. Chem. B*, 2021, **9**, 8321–8329.
13 Y. Jiao, L. Niu, S. Ma, J. Li, F. R. Tay and J. Chen, *Prog. Polym. Sci.*, 2017, **71**, 53–90.
14 E. Araya-Hermosilla, I. Moreno-Villoslada, R. Araya-Hermosilla, M. E. Flores, P. Raffa, T. Biver, A. Pucci, F. Picchioni and V. Mattoli, *Polymers*, 2020, **12**, 2017.
15 E. A. Araya-Hermosilla, M. Carlotti, F. Picchioni, V. Mattoli and A. Pucci, *Polymers*, 2020, **12**, 923.
16 R. Araya-Hermosilla, A. Pucci, E. Araya-Hermosilla, P. P. Pescarmona, P. Raffa, L. M. Polgar, I. Moreno-Villoslada, M. Flores, G. Fortunato, A. A. Broekhuis and F. Picchioni, *RSC Adv.*, 2016, **6**, 85829–85837.
17 E. Araya-Hermosilla, A. Giannetti, G. M. R. Lima, F. Orozco, F. Picchioni, V. Mattoli, R. K. Bose and A. Pucci, *Polymers*, 2021, **13**, 339.
18 E. Araya-Hermosilla, A. Gabbani, A. Mazzotta, M. Ruggeri, F. Orozco, V. Cappello, M. Gemmi, R. K. Bose, F. Picchioni, F. Pineider, V. Mattoli and A. Pucci, *J. Mater. Chem. A*, 2022, **10**, 12957–12967.
19 H. Bakhshi, H. Yeganeh and S. Mehdipour-Ataei, *J. Biomed. Mater. Res., Part A*, 2013, **101**, 1599–1611.
20 O. Makarova, P. Johnston, B. Walther, J. Rolff and U. Roesler, *Genome Announc*, 2017, **5**(33), e00793.
21 W. P. Mul, H. Dirkzwager, A. A. Broekhuis, H. J. Heeres, A. J. van der Linden and A. Guy Orpen, *Inorg. Chim. Acta*, 2002, **327**, 147–159.
22 D. Iacopini, J. Vančo, S. di Pietro, V. Bordoni, S. Zacchini, F. Marchetti, Z. Dvořák, T. Malina, L. Biancalana, Z. Trávníček and V. di Bussolo, *Bioorg. Chem.*, 2022, **126**, 105901.
23 T. Muhizi, S. Grelier and V. Coma, *J. Agric. Food Chem.*, 2009, **57**, 8770–8775.
24 S. Fortunato, C. Lenzi, C. Granchi, V. Citi, A. Martelli, V. Calderone, S. di Pietro, G. Signore, V. di Bussolo and F. Minutolo, *Bioconjugate Chem.*, 2019, **30**, 614–620.
25 B. Shirkavand Hadavand, M. Ataeefard and H. Fakharizadeh Bafghi, *Composites, Part B*, 2015, **82**, 190–195.